Adsorption geometry of sulfur on Ir(1 1 0)-c(2 4)S

Available online at www.sciencedirect.com
SCIENCE DIRECT®
Surface Science 539 (2003) L537–L541
SURFACE SCIENCE
www.elsevier.com/locate/susc

Surface Science Letters

Adsorption geometry of sulfur on Ir(1 1 0)-c(2 × 4)S

Jörg Kröger [a,*], Jens Kuntze [a], Andrea Atrei [b], Brunetto Cortigiani [c], Ugo Bardi [c], Gianfranco Rovida [c]

[a] *Institut für Experimentelle und Angewandte Physik, Christian-Albrechts-Universität zu Kiel, Leibnizstrasse 19, D-24098 Kiel, Germany*
[b] *Dipartimento di Scienze e Tecnologie Chimiche, Università di Siena, I-53100 Siena, Italy*
[c] *Dipartimento di Chimica, Università di Firenze, I-50129 Firenze, Italy*

Received 20 May 2003; accepted for publication 4 June 2003

Abstract

We investigate the Ir(1 1 0)-c(2 × 4)S adsorbate system using X-ray photoelectron diffraction. As proposed by a previous structure model based on a scanning tunneling microscopy experiment, we find that sulfur atoms of this superstructure enter the second adsorption layer. In contrast to the existing structure model the adatoms do not occupy on-top adsorption sites above first-layer adatoms. We refine the proposed structure model by moving sulfur atoms of the second adsorption layer out of the on-top position. Our experimental results are compared with single and multiple scattering calculations.

Keywords: X-ray scattering, diffraction, and reflection; Photoelectron diffraction; Surface structure, morphology, roughness, and topography; Adsorption kinetics; Sulphur; Iridium

The (1 1 0) surfaces of several face-centered cubic metals are known to exhibit reconstructions of the missing-row type, like Au(1 1 0) [1] and Pt(1 1 0) [2]. Based on low-energy electron diffraction (LEED) experiments for Ir(1 1 0) also a (1 × 2) missing-row reconstruction was believed to hold [3]. Investigations by scanning tunneling microscopy (STM) and helium atom scattering (HAS), however, revealed that the (1 1 0) surface stabilizes by formation of extended, oppositely tilted (3 3 1) facets [4–6].

Upon sulfur adsorption the faceted reconstruction is lifted and a (1 × 2) missing-row structure is induced instead [7]. A similar adsorbate-induced missing-row reconstruction was observed for alkali-metals on Cu(1 1 0), Ag(1 1 0) and Pd(1 1 0) [8]. At sulfur coverages of half a monolayer (ML) a p(2 × 2)2S superstructure develops where S atoms adsorb in zigzag chains along [$\bar{1}$ 1 0] with neighboring chains being in phase, i.e., the sulfur-sulfur distance along [0 0 1], which is the direction perpendicular to the chains, is always the same. At saturation coverage, which is reached at ≈0.75 ML, a c(2 × 4) superstructure was reported. The

* Corresponding author. Tel.: +49-431-880-3966; fax: +49-431-880-1685.
E-mail address: kroeger@physik.uni-kiel.de (J. Kröger).

0039-6028/03/$ - see front matter © 2003 Elsevier B.V. All rights reserved.
doi:10.1016/S0039-6028(03)00796-9

LEED pattern of this superstructure shows additional streaks at $\frac{1}{4}$ positions in the [$\bar{1}$ 1 0] direction whereas long-range order is missing along the [0 0 1] azimuth. For this overlayer the authors proposed that additional pairs of S adatoms, which they called dimers, enter the second adsorption layer and reside in on-top positions above first layer S atoms (see Fig. 1 where a schematic model of the proposed c(2×4) superstructure is displayed). The S dimers are ordered along the [$\bar{1}$ 1 0] direction whereas a long-range order along [0 0 1] is missing. From the adsorption energetics standpoint the on-top adsorption site appears to be unfavorable and thus the proposed structural model called for further experimental studies.

We were motivated by the open question concerning the sulfur adsorption geometry of sulfur-saturated Ir(1 1 0) and thus performed X-ray photoelectron diffraction (XPD) experiments on the adsorbate system Ir(1 1 0)-c(2×4)S. The main result of these investigations is a refined structure model: we confirm that sulfur atoms enter the second adsorbate layer and, in contrast to the previous STM investigation [7], occupy adsorptions sites, which slightly differ from on-top positions above sulfur atoms of the first layer.

XPD has become by now a quantitative tool for obtaining structure data. The dominant forward-scattering signals in XPD show up as clear signatures in angle distribution curves of core-level photoelectrons. Collecting electrons from a particular emission line, e.g., the S 2p line, we know that these electrons have their origin at the atom selected by the choice of the emission line in the spectrum. Thus the resulting diffraction patterns are element specific and show the corresponding atomic environment.

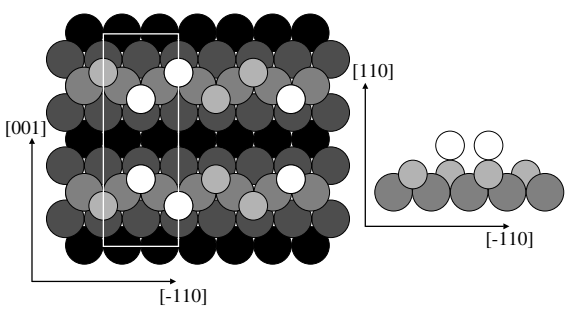

Fig. 1. Structure model of Ir(1 1 0)-c(2×4)S as proposed by a previous STM investigation [7] (left: top view, right: side view along [$\bar{1}$ 1 0]). The top view reveals Ir atoms of the top layer (grey circles), the second layer (dark-grey circles) and the third layer (black circles) in order to visualize the missing-row reconstruction along [$\bar{1}$ 1 0]. S atoms in the first adsorption layer (light-grey circles) and in the second adsorption layer (white circles) are depicted. The rectangle is added in order to reveal the c(2×4) superstructure. The side view along [$\bar{1}$ 1 0] (right panel) demonstrates the proposed on-top adsorption geometry (here only the top Ir layer is shown).

In the present work we use XPD as a structural method because the phase formed at saturation coverage of S on Ir(1 1 0) does not have long-range order [7]. This prevents the use of diffraction techniques such as LEED. On the other hand, XPD allows to verify in a straightforward way the model proposed on the basis of STM results.

The experiment was performed at room temperature and under ultrahigh-vacuum conditions with a base pressure of 5×10^{-9} Pa. For the XPD measurements the sample is illuminated by (non-monochromatized) MgKα X-rays ($h\nu = 1253.6$ eV). The binding energy scale was calibrated using a silver standard and setting the Ag $3d_{5/2}$ binding energy to 368.3 eV [9]. XPD curves were collected by measuring the S 2p (electron kinetic energy 1089 eV) and Ir $4f_{7/2}$ (electron kinetic energy 1192 eV) peak intensities as a function of the polar angle scanned along the [$\bar{1}$ 1 0] and [0 0 1] directions. The background was estimated by measuring the intensity at a point on the high kinetic energy side of the respective photoemission peaks. Our angle scans always show the constant background subtracted data. An experimental obstacle was the rather low cross-section for excitation of S 2p core level electrons, which we had to overcome by long measuring times and repeated scans of the same angle interval. The polar XPD curves were collected in a range of polar angles from $-10°$ to $70°$ due to limitations to the sample rotation in the experimental setup.

The Ir(1 1 0) surface was cleaned by repeated cycles of Ar^+ ion bombardments and subsequent annealing. Crystalline order was checked by LEED and cleanliness was monitored using X-ray photoelectron spectroscopy (XPS) and low-energy ion scattering (LEIS). Instead of using H_2S as in previous studies, the S chemisorbed phase was prepared by exposing the sample surface to the flux of

sulfur coming from pyrite (FeS_2) heated in a Knudsen cell [10,11]. Sulfur up-take was followed by means of LEIS, XPS and LEED. LEIS and XPS spectra measured for increasing exposures of the sample to the sulfur source indicate that sulfur adsorption reaches a saturation limit. The binding energy of the S 2p measured for this surface (162.7 eV) is in good agreement with the value reported for chemisorbed sulfur (162.7 eV [9]). No component corresponding to elemental sulfur was detectable above the noise level. The LEIS spectra for the clean surface and the sulfur saturated surface are shown in Fig. 2a and b, respectively. The peak due to sulfur is located at ≈620 eV. The sulfur saturated surface shows the c(2 × 4) LEED pattern with faint streaks observed in previous studies [7]. In order to find the orientation of the sample as mounted on the sample holder we acquired Ir $4f_{7/2}$ XPD curves for the clean surface.

In Fig. 3 we present the main result of this article: the upper curve shows the polar angle distribution curve of S 2p core level photoelectrons

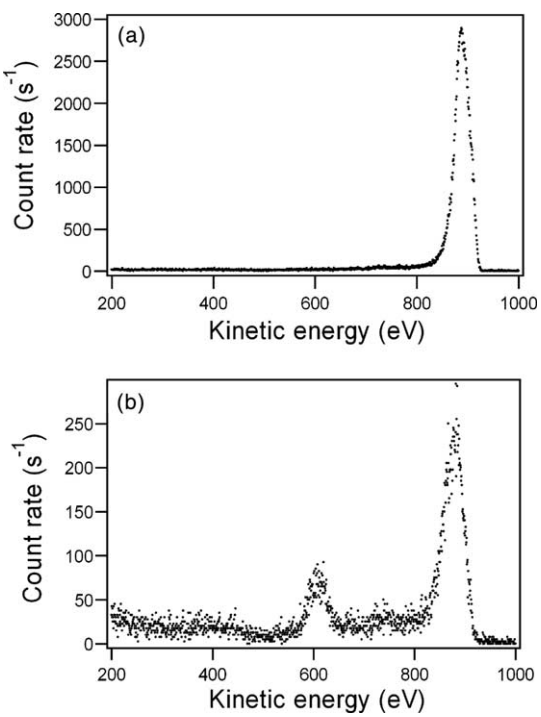

Fig. 2. (a) LEIS spectrum of clean Ir(1 1 0). (b) LEIS spectrum of sulfur-saturated Ir(1 1 0).

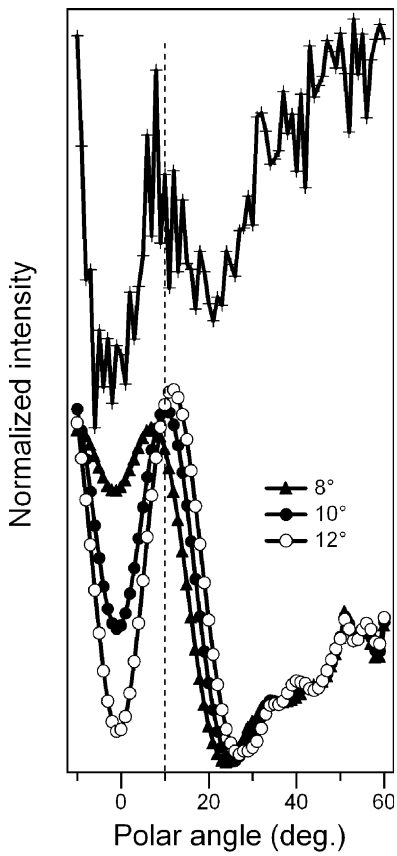

Fig. 3. Upper curve: polar angle distribution curve of S 2p core level photoelectrons of Ir(1 1 0)-c(2 × 4)S along [$\bar{1}$ 1 0]. A forward-scattering signal is observed at 10°. The anisotropy of this signal is ≈40%. A rise of the photoelectron intensity is also observed for negative angles. Lower curves: polar S 2p XPD curves as calculated using the single scattering cluster method for tilt angles of 8° (triangles), 10° (full circles), 12° (open circles) of the S dimers with respect to the sample normal. These curves were divided by the cosine of the polar angle in order to mimic the emission from a very thin overlayer.

along [$\bar{1}$ 1 0]. The data reveal a forward-scattering signal at 10°. The anisotropy of this peak (as defined by $(I_{max} - I_{min})/I_{max}$ with I_{max} and I_{min} being the intensities of the maximum and of the foot of the peak) is ≈40%. We interpret this forward-scattering peak as being due to neighboring sulfur atoms of the first and second adsorption layer. The axis connecting the centers of these adatoms is tilted by 10° with respect to [1 1 0]. This experimental result is in clear contrast with the structure model previously suggested by an STM investigation [7]:

the authors propose the above mentioned axis to be aligned with the [1 1 0] direction. The rise of intensity on the negative side of the polar angle interval is consistent with the fact that the negative and positive directions along the [$\bar{1}$ 1 0] azimuth are equivalent. Because of the limited range for the polar angle in the negative direction, the maximum of this forward-scattering peak is not visible on this side of the angle interval. The increase of intensity of the experimental XPD curve at higher (positive) polar angle is due to the fact that we have emission from a thin overlayer. Thus the intensity is roughly proportional to $(\cos(\theta))^{-1}$ (θ being the polar angle). We performed an analogous experiment for clean Ir(1 1 0), i.e., we set the detector of the analyzer to the core level energy of S 2p and acquired polar angle scans along [$\bar{1}$ 1 0]. As expected we obtained a featureless flat angle distribution curve (not shown). This result differs significantly from the polar angle scan displayed in Fig. 3 and thus we assign the observed signal to forward scattered photoelectrons of the S 2p core level. For analogous polar angle scans along other directions no intensity modulations of the S 2p photoelectrons were detectable above the noise level.

To confirm the interpretation of our XPD results, the experimental S 2p XPD curve was compared with calculations performed on the basis of the structure model given below (see Fig. 4). The results are given in the lower curves of Fig. 3 where for a series of tilt angles (8°, 10°, 12°) we plotted

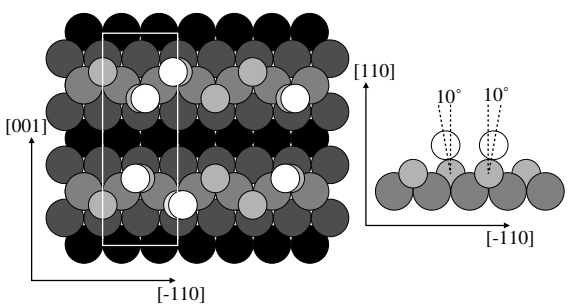

Fig. 4. XPD-based structure model of Ir(1 1 0)-c(2 × 4)S (left: top view, right: side view along [$\bar{1}$ 1 0], the assignment of colored circles to Ir and S atoms is the same as in Fig. 1). In contrast to the previously suggested model (see Fig. 1) the sulfur adatoms of the second layer are moved out of the on-top positions above first-layer adatoms. The corresponding tilting angle (refer to the side view in the right panel) is found to be 10°.

calculated XPD curves. The S–S and S–Ir bond lengths were chosen to be 2.1 and 2.4 Å, respectively. We performed calculations at the level of single scattering [12] and multiple scattering [13]. The sulfur and iridium phase shifts were derived from the muffin–tin potentials calculated for CdS and Ir crystals, respectively [13]. Test calculations carried out for the up-right position of sulfur adatoms of the first and second layer indicate no significant difference between the single scattering and multiple scattering S 2p polar XPD curves. Hence, the rest of the analysis was accomplished by means of the single scattering method. The calculations were performed on the basis of the model shown in Fig. 4 for a series of tilt angles with respect to the normal of the sample surface. Note that as the experimental XPD curve exhibits only a single peak the agreement between the experimental and the calculated polar angle distribution curves could exclusively judged from the matching of the position of the peak maximum. The uncertainty of the tilt angle was estimated on the basis of the variation of the tilt angle producing a significant difference with the experimental curve. In order to consider the fact that the S–S axis can be tilted by 10° and −10° with respect to [1 1 0] for each tilt angle the calculations were performed for the positive and the negative value. The resulting curves were then averaged prior to comparison with the experimental data. The best agreement with the experimental curve, as far as the forward-scattering peak position is concerned, is obtained for a tilt angle of (10 ± 2)°. The other features in the polar XPD curve can be attributed to higher order diffraction of the S 2p photoelectrons scattered by the outermost S atoms since these minor intensity modulations do not depend on the S adsorption site on the iridium surface. However, the experimental S 2p polar XPD curve is too noisy to allow a reliable determination of additional structure parameters such as the S–S bond length.

As a result, we obtain two facts. First, S atoms of this superstructure must reside in the second adsorption layer, which confirms the suggestion of the previous STM investigation [7]. If only one adsorption layer was present one would expect forward scattered photoelectrons only at grazing emission angles with respect to the sample surface.

Second, since we observe a forward-scattering signal at 10° with respect to the sample normal the sulfur adatoms of the second layer are not in on-top positions above first layer adatoms. Rather than being aligned along [1 1 0], the S adatoms are moved out of the on-top position and are aligned with S adatoms of the first layer along a direction, which is tilted by 10° with respect to the surface normal. As a consequence we propose a refined structure model, which is displayed in Fig. 4. Compared with the previously suggested structure model (refer to Fig. 1) the centers of the spheres of first-layer and second-layer adatoms are thus separated by $\approx$0.3 Å along [$\bar{1}$ 1 0]. A possible reason for the tilting of the S dimers could be the steric repulsion between S atoms.

In summary, we demonstrated by means of XPD that for the adsorbate system Ir(1 1 0)-c(2 × 4)S sulfur atoms enter the second adsorption layer and reside in adsorption sites which are close to the on-top positions above first-layer adatoms. The polar angle distribution curves along [$\bar{1}$ 1 0] of S 2p core level electrons exhibit a forward-scattering signal at 10°. As a consequence sulfur adatoms of the second layer reside in adsorption sites which differ from the on-top position by 0.3 Å along [$\bar{1}$ 1 0].

Acknowledgements

Fabrication of the sulfur crucible by W. Krüger (Kiel) and advice how to handle it by C. Kreis (Kiel) are gratefully acknowledged. The work was partially financed by MIUR and DAAD (VIGONI).

References

[1] W. Moritz, D. Wolf, Surf. Sci. 88 (1979) L29, 163 (1985) L655;
J. Möller, H. Niehus, W. Heiland, Surf. Sci. 166 (1986) L111;
K.M. Ho, K.-P. Bohnen, Phys. Rev. Lett. 59 (1987) 1833;
M. Copel, T. Gustafsson, Phys. Rev. Lett. 57 (1986) 723.
[2] P. Fery, W. Moritz, D. Wolf, Phys. Rev. B 38 (1988) 7275;
T. Gritsch, D. Coulman, R.J. Behm, G. Ertl, Phys. Rev. Lett. 63 (1989) 1086.
[3] C.-M. Chan, M.A. Van Hove, Surf. Sci. 171 (1986) 226.
[4] R. Koch, M. Borbonus, O. Haase, K.H. Rieder, Phys. Rev. Lett. 67 (1991) 3416.
[5] W.F. Avrin, R.P. Merrill, Surf. Sci. 274 (1992) 231.
[6] J. Kuntze, S. Speller, W. Heiland, Surf. Sci. 402 (1998) 764.
[7] J. Kuntze, S. Speller, W. Heiland, Phys. Rev. B 62 (2000) 4681.
[8] B.E. Hayden, K.C. Prince, P.J. Davies, G. Paolucci, A.M. Bradshaw, Solid State Commun. 48 (1983) 325;
R. Schuster, J.V. Barth, G. Ertl, R.J. Behm, Surf. Sci. Lett. 247 (1991) L229.
[9] J. Chastain (Eds.), Handbook of X-Ray Photoelectron Spectroscopy, Perkin-Elmer Corporation, Physical Electronics Division, 6509 Flying Cloud Drive, Eden Prairie, Minnesota 55344, 1992.
[10] M. Traving, Ph.D. Thesis, University of Kiel, 1999.
[11] C. Kreis, M. Traving, R. Adelung, L. Kipp, M. Skibowski, Appl. Surf. Sci. 166 (2000) 17.
[12] C.S. Fadley, in: R.Z. Bachrach (Ed.), Synchrotron Radiation Research: Advances in Surface Science, Plenum, New York, 1991.
[13] Y. Chen, M.A. Van Hove. Available from <electron.lbl.gov/mscdpack>.